Al-Qadisiyah J. Vet. Med. Sci. 2025; 24 (3): 10.29079/qjvms.2025.166349.1130
The 1st National and International Scientific Conference November 26 / 2025
ISSN P: 1818-5746
E: 2313-4429
qjvms.qu@edu.iq

Anatomical, Histological, and Histochemical Characterization of the Tracheobronchial Tree in the Euphrates Jerboa (*Allactaga euphratica*)

Alaa Sameer [1] Abdulrazzaq B. Kadhim [2]
Department of Anatomy and Histology, College of Veterinary Medicine, University of Al-Qadisiyah, Iraq
https://orcid.org/0000-0001-6356-4223 [2]

Submitted: October 17, 2025
Revised: October 10, 2025
Accepted: November 11, 2025

Correspondence:
Alaa Sameer
vet.post24.44@qu.edu.iq

Abstract The Euphrates jerboa, Allactaga euphratica, is a rodent which has adapted to life in a desert, and whose respiratory system is specialized to resist with dusty and inhospitable surroundings. This research sought to elaborate the anatomy, histomorphology, and histochemistry of the jerboa's trachea and bronchial tree through gross dissection and examination, resin casting, and routine histological staining. In total, fifteen adult male jerboas were separated into equal groups of anatomy, casting, and histology. In anatomical terms, the jerboa's trachea was a short, flexible tube with an average length of 0.7 ± 0.32 cm and was comprised of eight cartilaginous rings shaped like the letter 'C'. The right primary bronchus was more branched than the left one, with the right forming a cranial, caudal, and accessory bronchus, and the left bronchus branching into three major branches. The resin casting gross and illustrated this asymmetry and the bronchial pattern which was efficient and presumably enhances the ventilation. Histology of the trachea illustrated four layers in the wall: the mucosa, submucosa, cartilage, and adventitia. Pseudostratified ciliated columnar epithelium with intermixed goblet cells covering a vascular lamina propria lined the tracheal mucosa; the submucosa had seromucous glands and connetive tissue. The perichondrium of the tracheal rings was composed of hyaline cartilage. They were separated dorsally and completed by the trachealis smooth muscle and elastic fibers. Lymphocytes and macrophages were diffuse in the lamina propria–submucosa indicating the presence of mucosal immune surveillance. The results obtained probably indicate extensive adaptation of the Euphrates jerboa to the desert, respiratory adaptations such as having a shortened airway, a mucus-covered epithelium, and asymmetrical bronchi to an extent where gas exchange is mucus protected and gas environmental particulates. The overall lower respiratory system, exemplifies evolution desert evolution.

Keywords: Anatomy, Bronchial tree, Histochemistry, Jerboa, Trachea

Introduction The conducting airways offer a unique mucociliary barrier that conditions the inspired air and protects the airways from the first line of defence against particulates and pathogens (1). Irrespective of the cause of the airway disease, epithelial junctions, ciliary function, and secretory balance (goblet cells/submucosal glands) dysregulation disruption of dysregulated repair injury interface modulation emphasize how modern reviews (2). Developmental and morphogenetic programs find the scale aspect of the hallmark architecture characteristic of the trachea (C-shaped, ventrolaterally positioned hyaline cartilage rings with a dorsal trachealis band) that s, with dysregulated repair, form the hallmark architecture of the Scale (3-5). The respiratory epithelium has the capacity to differentiate between viral and non-viral aggressors and to orchestrate downstream responses that drive the development of airway disease; the weakened epithelial interferon action exponentially enhances risk of exacerbations and continues to drive the inflammation cycle (1,6,7). Goblet-cell activity is influenced by cholinergic and cytokine signals, and muscarinic antagonists can secondarily reduce mucus hypersecretion (1,8). In our jerboa trachea, histomorphology illustrates, epithelial-immune-mechanical integration, the pseudostratified ciliated epithelium with poorly developed goblet cells. That covers a thin lamina propria with dispersed lymphoid cells, while the hyaline cartilage rings and the dorsal

Al-Qadisiyah J. Vet. Med. Sci. 2025; 24 (3): 10.29079/qjvms.2025.166349.1130
The 1st National and International Scientific Conference November 26 / 2025
ISSN P: 1818-5746
E: 2313-4429
qjvms.qu@edu.iq

trachealis maintain the patency and compliance of the lumen to trachea (7).Recent non-model mammal accounts confirm classic features of the respiratory system—pseudostratified ciliated epithelium, rings incomplete in the dorsal region, asymmetric right–left bronchial system—while describing lobe structure and gland distribution that are species- and ecology-dependent (9, 10). According to this, a detailed histomorphological study of the jerboa trachea and bronchi can reveal adaptations to dry climates (e.g. mucus economy, ciliary density, gland abundance) and set standards for both comparative anatomy and applied airway engineering.

Materials and Methods

Ethical approval

The project was approved (2257 in 2/9/2024) by the Committee for Research Ethics at the College of Veterinary Medicine, University of AL-Qadissiyah, Iraq.

Experimental Animals

We collected 15 healthy adult male Euphrates jerboas (Allactaga euphratica), clinically normal and without respiratory disorders, during the summer season in Diwaniya Province, Iraq. The animals were kept in a temperature-controlled laboratory (22–25 °C, 12 h light/dark cycle) and were provided with ad libitum food and water prior to euthanasia. All procedures pertaining to the animals were in compliance with the established humane protocols issued by the College of Veterinary Medicine of the University of Al-Qadisiyah. Animals stayed for 14 days before scarification.

Experimental Design

In order to study different analytical approaches, the animals were randomly separated into 3 equal groups (n = 5 per group):

Group I

Anatomical study of the trachea and lungs.

Group II

Bronchial tree casting for visualization of the bronchial branching pattern.

Group III

Histological and histochemical evaluations of the trachea and primary bronchi.

Anatomical Examination

Each animal underwent anesthesia, according to ethical protocols of the laboratory. The ventral cervical as well as thoracic compartments were methodically opened to reveal the trachea, lungs, and subordinate thoracic organs and systems while preventing injury to the overlying structures. Topographic position of the trachea was recorded in position, prior to specimen collection.

The trachea was carefully removed from the cricoid cartilage to the point of bifurcation at the level of the fourth thoracic vertebra. Morphometric parameters recorded included total tracheal length (mm), dorsoventral and laterolateral diameter (mm), as well as the total number of bronchi. The body and trachea were weighed on a precision analytical balance (Sartorius 1212 MP, Germany) and the data expressed as mean ± standard error.

Corrosion Cast Technique of the Bronchial Tree

Five adult jerboas were placed in Group II made to do the selected for the preparation of the resin cast, in order to study the pattern of the branches bronchi. After the animals were processed, the larynx, trachea, and lungs were very carefully separated as a block with the covering connective tissue, to prevent casting material from leaking.

The four-mm cannula was inserted through the larynx and tied with surgical stitching. The Pyrax Rapid Repair acrylic resin (Pyrax Pollars, Roorkee, India) was prepared per the manufacturer's guidelines to achieve the recommended working viscosity. The resin was then placed at a steady rate and using a 20mL syringe and in 1.0, 1.25, 1.5, 1.75, and 2.0mL aliquots with light manual pressure. The cannula was gently clamped with forceps so that the cannula would not reflux after the resin was applied.

Specimens were immersed in the medium, which was allowed to cure overnight at 25-30 degrees C. They were then transferred to 40% KOH at room temperature (20 degrees C/warm room) for tissue maceration for 4-5 days (changing the solution every day). The remnants of casts were then rinsed for 60 min under running tap water, blotted, and air dried on absorbent paper until casts became rigid and subsequently, they were stereomicroscopically examined (7-80×) in oblique and ring-light illumination for enhanced relief imaging. A scale bar was added later on during post-processing using a staging micrometer. Using the stereomicroscope, the bronchial orientation is tracheobronchial in multi-view (with scale bars, bronchial and segment lengths, branching diameters, branching order and angles, etc.) and the measurements were done in ImageJ/Fiji. 3D focus stacking was performed when the depth of field required was more than available.

Histological and Histochemical Study

Five jerboas (Group III) were processed for trachea and bronchial specimens. Upon completion of the sample collection, tissues from the cranial, middle and caudal located regions of the trachea and also from the left and right principal bronchi were obtained. The samples were preserved for 48 hours in 10 percent neutral buffered formalin at 1:10 (tissue to fixative) ratio. The samples were left in running tap water for 4-6 hours, and afterward underwent the standard graded ethanol dilutions. Dewaxing in xylene was followed by embedding in

Al-Qadisiyah J. Vet. Med. Sci. 2025; 24 (3): 10.29079/qjvms.2025.166349.1130
The 1st National and International Scientific Conference November 26 / 2025
ISSN P: 1818-5746
E: 2313-4429
qjvms.qu@edu.iq

paraffin wax. 5µm thick sections were obtained from the paraffin blocks with a rotary microtome and were placed onto glass slides. General histological structure was prepared for using routine staining with hematoxylin and eosin (H&E), and then by the Periodic Acid- Schiff (PAS) reaction to study the presence of neutral mucopolysaccharides in goblet cells and glands. An Olympus light microscope (BX-series, Japan) fitted with a digital camera was used for microscope imaging and observation.

Statistical analysis

Morphometric results were subjected to a two-way analysis of variance (ANOVA) in order to determine the change in the assessed parameters. Data are given as mean ± standard error, and results were deemed significant at $P \leq 0.05$.

Results

Topography and Gross Morphology of the Trachea.

The trachea of the Euphrates Jerboa starts from the larynx at the level of the cricoid cartilage, descends the neck ventral to the esophagus, and enters the thorax where it divides to the right and left bronchi at the level of the 4th thoracic vertebra (figure 1–2). The right and left bronchi are the primary bronchi. As the trachea descends, it maintains a series of open dorsal C-shaped rings of cartilage, the dorsal gap of each of these rings being closed by the trachealis muscle and the fibroelastic membrane. The fibroelastic rings join adjacent cartilage and these structures permit the trachea to stretch and allow for minor diameter reductions during inspiratory and swallow cycles, permitting gas exchange and ventilation.

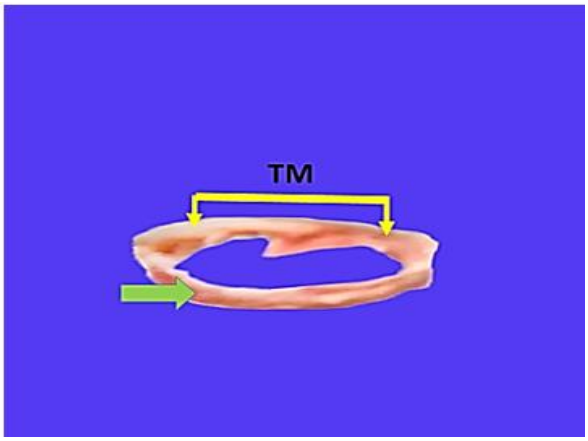

Figure 1: Euphrates jerboa tracheal rings. The dorsal view shows the dorsal margin ring hyaline cartilage rings strung together with tracheal muscle. This construction maintains the airway's ease of access while still allowing free movement of the head.

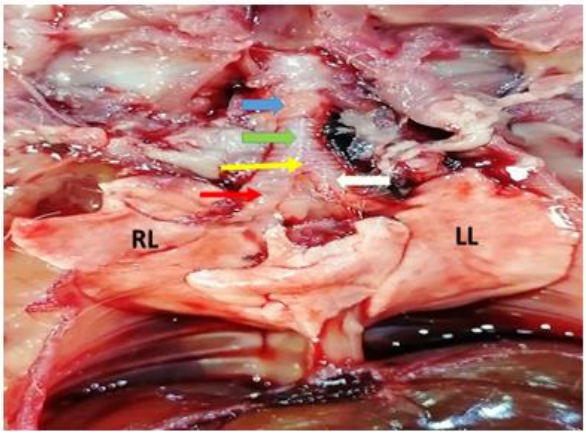

Figure 2: Trachea and lungs within the thoracic cavity. The image shows the larynx, trachea, and laryngeal bifurcation into the right and left bronchi. The right and left lungs' lobes and their relations with the heart and diaphragm are also displayed. Arrows: Blue: Cranial (cervical) trachea, Green: Mid-trachea (thoracic), C-shaped rings visible, Yellow: Distal trachea just proximal to the carina, Red: Right primary (main) bronchus, White: Left primary (main) bronchus. The jerboa trachea measured 7.0 ± 3.2 mm in length (mean ± SD, n = X; range Y–Z mm) and contained 8 (7–9) cartilage rings. The outer cartilage diameter averaged 5.0 ± 0.6 mm (range A–B mm). No difference in tracheal length was detected between males and females (t-test, t = …, P = 0.27). Throughout the cervical and thoracic regions, the diameter of the trachea is almost uniform, only narrowing slightly toward the carina. The lungs visually and constitutionally differ in both shape and volume; the right lung has four lobes (cranial, middle, caudal, and accessory) while the left lung has two lobes (cranial and caudal) (Fig. 3–5).

Al-Qadisiyah J. Vet. Med. Sci. 2025; 24 (3): 10.29079/qjvms.2025.166349.1130
The 1st National and International Scientific Conference November 26 / 2025
ISSN P: 1818-5746
E: 2313-4429
qjvms.qu@edu.iq

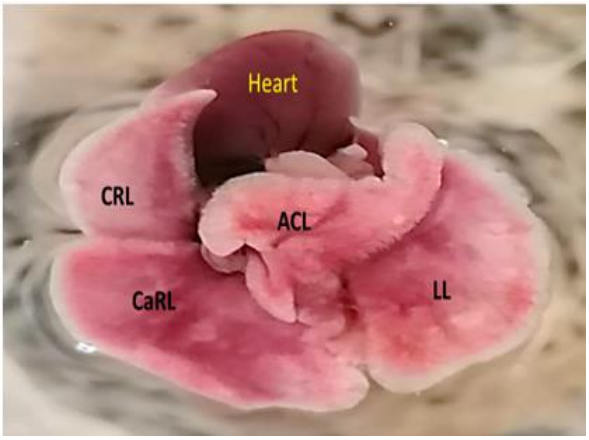

Figure 3: Lobules of lungs. The right lung possesses cranial, caudal, and accessory lobes, while the left lung has two principal lobes. This asymmetry is a consequence of the organization of the thoracic cavity.

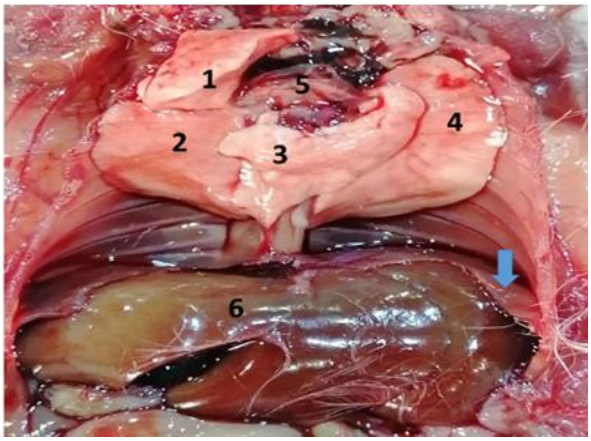

Figure 4: The Ventral view of the lungs in relation to the thoracic organs. This illustration shows the lungs in relation to the heart, liver, and diaphragm. The clear separation of the lobes indicates the structural organization in the thoracic cavity. Blue arrow: the diaphragm (right costal/ventral margin)

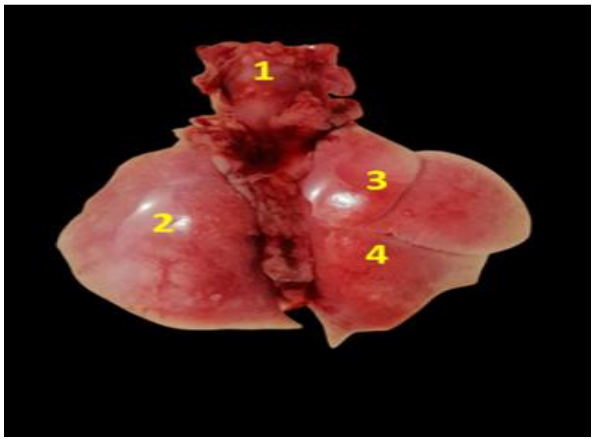

Figure 5: The costal view of the lungs and the trachea. The trachea is seen branching off into the right and left bronchi which then enter their respective lobes. The drastic difference in right and left sides of the lung is a notable example of asymmetry.

Corrosion Cast Findings of the Bronchial Tree

The bronchial tree produced from resin casting showed clear divisions of the tracheobronchial system (Fig. 6, Fig. 7). At the level of the fourth thoracic vertebra, the trachea bifurcated into the left and right main bronchi.

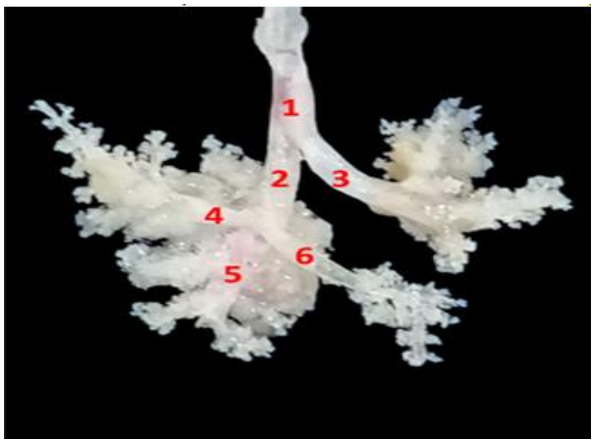

Figure 6: A resin cast of the bronchial tree of the Euphrates jerboa. This illustrates the trachea bifurcating into right and left principal bronchi plus primary, secondary, and accessory branches. The branching pattern reveals ordered air allocation to the lung lobe.

Al-Qadisiyah J. Vet. Med. Sci. 2025; 24 (3): 10.29079/qjvms.2025.166349.1130
The 1st National and International Scientific Conference November 26 / 2025
ISSN P: 1818-5746
E: 2313-4429
qjvms.qu@edu.iq

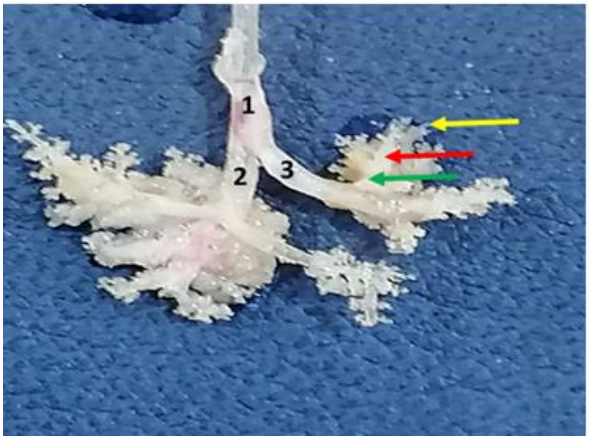

Figure 7: Cast of the bronchial and bronchiolar tree, bronchi showed in red and segmental in blue. This figure delineates the level from the trachea through the terminal bronchi and alveolar zones. Directional primary, secondary, and tertiary bronchi in the figure are shown with colored coded arrows.

The right main bronchus has been noted to arise from the trachea. Apart from the rest, it is also slightly wider and longer. The right bronchus gives rise to three primary bronchi: cranial, caudal, and accessory. The bronchi forming the dense network of bronchioles leading to the alveolar region are known as the caudal and cranial tertiary bronchi, while the accessory bronchus is aimed for the accessory lobe of the right lung.

The left principle bronchus was also more deficient than the right in length and also in diameter. It gave rise to three primary bronchi, each of which branched into several secondaries and tertiaries which then ended in terminal bronchioles and alveoli. The left lung also had bronchi which were more terminal than those on the right, the overall elaboration of the bronchial tree in the left lung was less complex than on the right.

Histological Structure of the Trachea

The examination of the tissue under a microscope showed that the wall of the trachea was made of four layers: the mucosa and the submucosa, and the cartilage, which includes the layer of muscle, and the layer of adventitia (fig. 8–10).

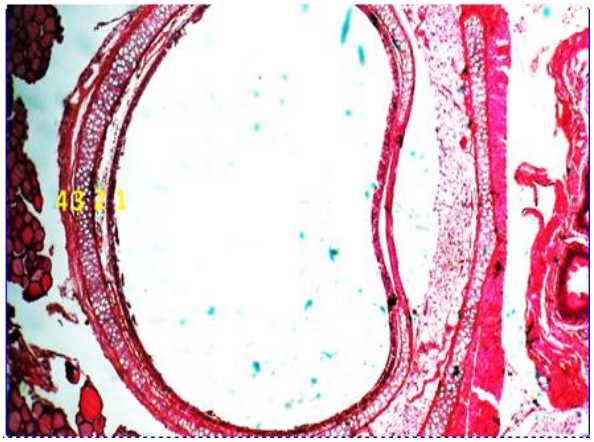

Figure 8: Histological section of the trachea, H&E, ×4. This section shows the pseudostratified ciliated columnar epithelium, submucosa, cartilage ring, and adjacent connective tissue, which comprise the tracheal wall, PSC, and the basic construct of the tracheal wall.

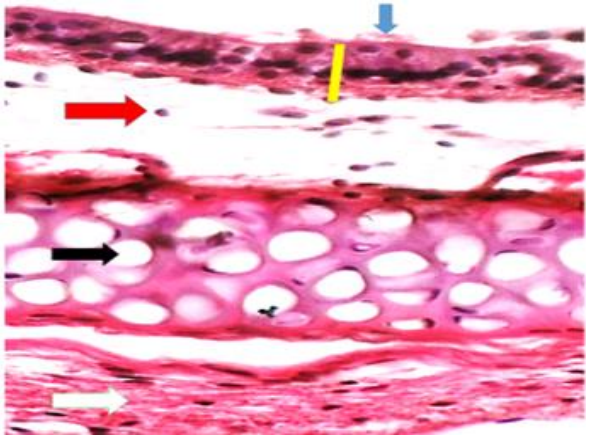

Figure 9: Section of the trachea shown under higher magnification, H&E, ×100. Visible in the lamina propria and submucosa are the ciliated epithelial cells and goblet cells. The mucosa structure allows for efficient mucociliary transport due to the mucosa supportive structures.

Al-Qadisiyah J. Vet. Med. Sci. 2025; 24 (3): 10.29079/qjvms.2025.166349.1130
The 1st National and International Scientific Conference November 26 / 2025
ISSN P: 1818-5746
E: 2313-4429
qjvms.qu@edu.iq

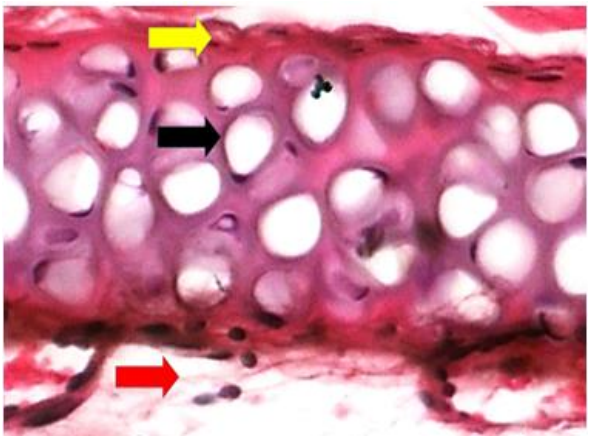

Figure 10: Tracheal cartilage and the adventitial layer, H&E, ×40. The hyaline cartilage which contains chondrocytes in lacunae is encircled by the perichondrium. The perichondrium is connected to the trachea via connective tissue and blood vessels due to the adventitia's anchoring position. Arrows: Yellow: Perichondrium (fibrous layer) over the cartilage, Black: Chondrocyte within a lacuna in hyaline cartilage, Red: Submucosa with seromucous gland acini/ducts. Tunica mucosa: The inner mucosal surface was lined with pseudostratified ciliated columnar epithelium and with three cell types—ciliated columnar cells, goblet, and basal cells. The ciliated cells were tall and slender with numerous motile cilia in the lumen. Goblet cells were numerous and contained mucin granules positively stained with PAS stain which meant neutral mucopolysaccharides were present (Fig. 11). Basal cells were small, triangular, and resting on the basement membrane and did not reach the lumen surface. The lamina propria was made of loose connective tissue composed of fine collagen fibers, small blood vessels, and some immune cells which included lymphocytes and macrophages.

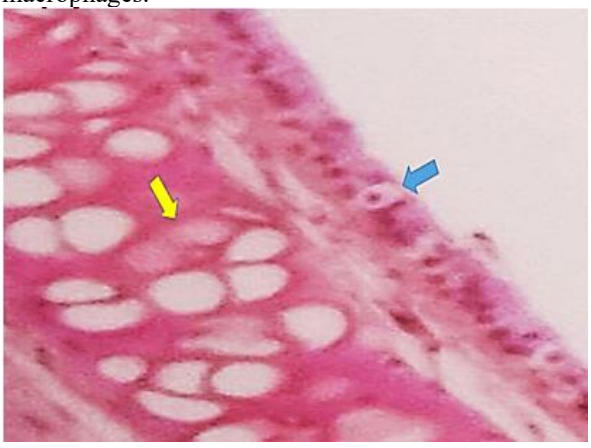

Figure 11: Tracheal section PAS stained to demonstrate goblet cells, ×400. There are goblet cells filled with magenta stained mucin situated amongst ciliated columnar cells. The PAS reaction illustrates secretion of neutral mucopolysaccharides, which airway epithelium uses for protective function. Arrows: Yellow: Hyaline cartilage of the tracheal ring (chondrocytes in lacunae). Blue: Respiratory epithelium—pseudostratified ciliated columnar; the cell indicated is a goblet cell in the mucosa.

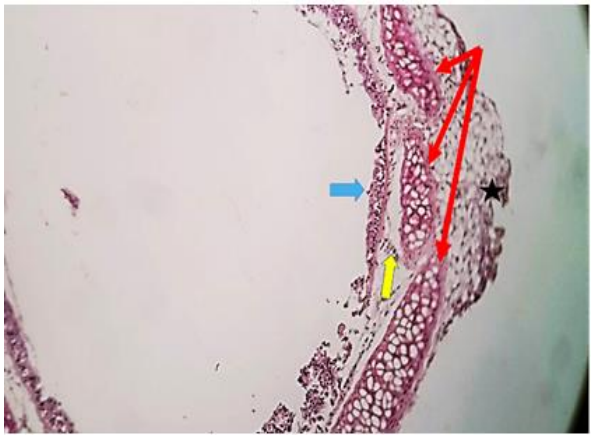

Figure 12: Histological section of a bronchus. (×4. HE). The bronchial wall consists of a pseudostratified ciliated columnar epithelium, submucosal connective tissue with mucus glands, and broken pieces of cartilage. These elements show a progressive changes from trachea to bronchus anatomy. Red arrows: Hyaline cartilage rings (C-shaped). Blue arrow: Trachealis smooth muscle spanning the dorsal gap between ring ends. Yellow arrow: Lamina propria / inner perichondrium (fibroelastic tissue between mucosa and cartilage). Black star: Adjacent esophageal wall/soft tissue dorsal to the trachea.Cartilaginous layer: The rings of the trachea were constructed from the cells of hyaline cartilage having chondrocytes enclosed in lacunae surrounded by amorphous extracellular matrix. The perichondrium containing fibroblasts and elastic fibers bordering the cartilage ring and merging with the submucosa and adventitia.Tunica adventitia: The innermost layer was constructed of loose connective tissue with blood vessels and tiny nerves that served to anchor the trachea to the surrounding structures. The bronchus internal structure was composed of a primary bronchi and secondary bronchi. The internal structure of tendency for structural modifications to occur. The bronchi remained lined with primary bronchi and secondary bronchi. The bronchus with the densest vascularization was the very first and served as a primary bronchi. Its internal structure had the most developed epithelial lining and a pseudostratified ciliated columnar gastro- bronchial. The submucous was

Al-Qadisiyah J. Vet. Med. Sci. 2025; 24 (3): 10.29079/qjvms.2025.166349.1130
The 1st National and International Scientific Conference November 26 / 2025
ISSN P: 1818-5746
E: 2313-4429
qjvms.qu@edu.iq

chemical-neutral brown. Great tubules on the side of the porous of the waxy, brown, cream and magenta tissue. The hilum of the left lung served for the bronchial roots and bronchus emerging in the lung. Fine collaterals made of dense connective tissue served for the bronchus to hilum of the left lung. The decrease in bronchi submucosa and fibrous bronchi to bronchioles was symmetric with less profusion of mucus. The mechanic increased the force and speed.

Discussion

In this study, the Euphrates jerboa has a trachea comprising about 8 C-shaped cartilaginous rings of comparatively uniform lumen diameter. This seems to be consistent with the Delaware basin of the Mamma region of the Euphrates (7), although differences in the number and completeness of rings are also quite common (11). For example, in ring number and cartilage thickness, the variations in the dorsal membrane of comparative airways are said to be the result of different respiratory and mechanical requirements (12, 13). This is consistent with other mammals in which the bronchus on the same side of the body as the bronchus bifurcates and serves several lobes (14). In large mammals and rodent species, this asymmetry is viewed as a result of the position of the thoracic organs and the differing volume requirements of the lobes (15). Our corrosion casts illustrate that euphratica possesses a right bronchus which branches into a singular, distinctly accessory bronchus. This is parallel to the accessory lobular bronchi of rodents and smaller mammals (16). This morphology may improve ventilation especially with preferential perfusion to larger lung lobes. This is greater than the comparative studies which describe consolidation of bronchial branches and the quanta of bronchial systems as a function of interspecies and bronchial system functional factors (12,17).

To the sample histological examination, the airway submucosa of the jerboa exhibits a notable abundance of goblet cells, especially considering the relative scarcity of submucosal glands. In comparative airway models, the ratio of often differs among species and regions of the airway; animals inhabiting environments frequently enhance surface secretory cells (13,18). More recent mechanistic work in the airway of rodents and humans has documented ciliated and secretory cell distributions that are peculiar to the species and are strongly associated with the effectiveness of mucociliary clearance (19). In A. euphratica, the predominance of epithelial goblet secretion may be an adaptive compromise (20, 21). The reduction of cartilage in the terminal bronchioles is thought to be in response to the need for airway flexibility during dynamic ventilation, while still allowing for the maintenance of patency in the presence of negative pressures (21,22). The presence of a relatively thick connective adventitial layer provides support for the anchoring and blood supply, as noted in the airways of rodents and smaller mammals (12).

The construction of airways in jerboas is matched, in form and function, to the needs of a desert environment, with a short and stable tracheal tube, asymmetric 'balanced' ventilation, and a 'defensive' epithelium that spares water (9). Considered sequence modulations of epithelium and ciliation in different species, then, functionally adapted to respiratory rates and other eco-physiological variables (19, 23).

Conclusion

To conclude, the tracheobronchial system of the Euphrates jerboa is fundamentally mammalian in design but reveals adaptive changes for life in the desert. The trachea is relatively short and consists of C-shaped hyaline cartilage rings joined by fibromuscular tissue, which provides rigidity and flexibility for breathing. The right bronchus is more branched than the left, which serves efficient ventilation of the bigger right lung lobes. The respiratory mucosa is histologically covered by a thin layer of the pseudostratified ciliated columnar epithelium and goblet cells with sparse submucosal glands. This suggests an efficient protective system which conserves water while maintaining airflow with mucociliary clearance.

Funding

The study was self-funded. No external grants or sponsorships supported this work.

Acknowledgement

The authors would like to thank the College of Veterinary Medicine, University of Al-Qadisiyah, Iraq, for facility access.

Conflict of Interest

No conflict of interest is declared by the authors

References

1. Raby Katie Louise; Michaeloudes Charalambos; Tonkin James; Chung Kian Fan; Bhavsar Pankaj Kumar. Mechanisms of airway epithelial injury and abnormal repair in asthma and COPD. Frontiers in Immunology. 2023;14:1201658. https://doi.org/10.3389/fimmu.2023.1201658
2. Kishimoto Keishi; Morimoto Mitsuru. Mammalian tracheal development and reconstruction: insights from in vivo and in vitro studies. Development. 2021;148(13):dev198192. https://doi.org/10.1242/dev.198192
3. Iber Dagmar; Mederacke Malte. Tracheal ring formation. Frontiers in Cell and Developmental

Biology. 2022;10:900447. https://doi.org/10.3389/fcell.2022.900447
4. Nawroth Janna C.; van der Does Anne M.; Ryan Firth Amy; Kanso Eva. Multiscale mechanics of mucociliary clearance in the lung. Philosophical Transactions of the Royal Society B: Biological Sciences. 2020;375(1792):20190160. https://doi.org/10.1098/rstb.2019.0160
5. Cao Yu; Chen Miao; Dong Dan; Xie Songbo; Liu Min. Effects of air pollutants on cilia movement: review of the mechanism. Thoracic Cancer. 2020;11(3):505-510. https://doi.org/10.1111/1759-7714.13323
6. Frey Anne; Lunding Lisa P.; Ehlers Jan-Christian E.; Weckmann Ulrich; Zissler Ulrich M.; Wegmann Marcus. More than just a barrier: airway epithelial cells-immune cell interactions in asthma. Frontiers in Immunology. 2020;11:761. https://doi.org/10.3389/fimmu.2020.00761
7. Guo-Parke Hong; Linden Dermot; Weldon Sinéad; Kidney Joseph C.; Taggart Clifford C. Deciphering respiratory-virus-associated interferon signaling in COPD airway epithelium. Medicina (Kaunas). 2022;58(1):121. https://doi.org/10.3390/medicina58010121
8. Calzetta Luigino; Ritondo Beatrice Ludovica; Zappa Maria Cristina; Manzetti Gian Marco; Perduno Andrea; Shute Janis; Rogliani Paola. The impact of long-acting muscarinic antagonists on mucus hypersecretion and cough in chronic obstructive pulmonary disease: a systematic review. European Respiratory Review. 2022;31(164):210196. https://doi.org/10.1183/16000617.0196-2021
9. Pantoja Bruna Tássia Santos; Marques Silva Armando Reinaldo; Mondêgo-Oliveira Renata; Santos Silva Thamires; Carvalho Marques Babara; Pontes Albuquerque Rafaela; Cortez Sá Sousa Joicy; Grassi Rici Rose Eli; Miglino Maria Angélica; Lislea Sousa Alana; Resende Franciolli André Luís; Martins Sousa Eduardo; Abreu-Silva Ana Lúcia; Cardoso Carvalho Rafael. Morphological study of larynx, trachea, and lungs of Didelphis marsupialis (Linnaeus, 1758). Veterinary World. 2020;13(10):2142-2149. https://doi.org/10.14202/vetworld.2020.2142-2149
10. Yeou Se Hyun; Shin Yoo Seob. Tissue-engineered tracheal reconstruction. Biomimetics. 2025;10(7):457. https://doi.org/10.3390/biomimetics10070457
11. Adams DR, Dellmann HD. Respiratory system. In: Textbook of Veterinary Histology. 5th ed. Philadelphia: Lippincott Williams & Wilkins; 1998.
12. Abidu-Figueiredo M, Xavier-Silva B, Cardino M, Babinski M, Chagas M. Celiac artery in New Zealand rabbit: anatomical study of its origin and arrangement for experimental research and surgical practice. Pesquisa Veterinária Brasileira. 2008;28(5):267-272. https://doi.org/10.1590/S0100-736X2008000500002
13. Aitken ML, Villalon M, Pier M, Verdugo P, Nameroff M. Characterization of a marker of differentiation for tracheal ciliated cells independent of ciliation. American Journal of Respiratory Cell and Molecular Biology. 1993;9:26-32. https://doi.org/10.1165/ajrcmb/9.1.26
14. Aitken ML, Villalon M, Pier M, Verdugo P, Nameroff M. Characterization of a marker for tracheal basal cells. Experimental Lung Research. 1995;21:1-16. https://doi.org/10.3109/01902149509031741
15. Al-Abasi RJ, Mirhish SM. Anatomical and histological study on the trachea and lung of one-humped camel in middle of Iraq. MSc thesis. College of Veterinary Medicine, University of Baghdad; 2001.
16. Al-Anbaki AA. Anatomical, histological, and radiological study of trachea and lungs in domestic rabbits. MSc thesis. College of Veterinary Medicine, University of Baghdad; 2013.
17. Albertin KH. Respiratory system blood supply of caudal mediastinal lymph node in sheep. Anatomical Record. 1980;212(2):129-131. https://doi.org/10.1002/ar.1092120205
18. Albertine KH, Wiener-Kronish JP, Roos PJ, Staub NC. Structure, blood supply, and lymphatic vessels of the sheep visceral pleura. American Journal of Anatomy. 1982;165:277-294. https://doi.org/10.1002/aja.1001650305
19. Amiri MH, Gabella G. Structure of the guinea pig trachea at rest and in contraction. Anatomy and Embryology (Berlin). 1988;178(5):389-397. https://doi.org/10.1007/BF00306045
20. Amis TC, McKiernan BC. Systemic identification of end bronchial anatomy during bronchoscopy in the dog. American Journal of Veterinary Research. 1986;47(12):2649-2627. https://doi.org/10.2460/ajvr.1986.47.12.2649
21. Aspinall V, Capello M, Japery A. Introduction to Veterinary Anatomy and Physiology. 2nd ed. London: Butterworth Heinemann, Elsevier; 2009. p. 90-96.
22. Aughey E, Frye FL. Comparative Veterinary Histology with Clinical Correlates. 1st ed. London: Manson Publishing Ltd; 2001. https://doi.org/10.1201/b15184

23. Baba MA, Choudhary AR. Histomorphology of the pulmonary alveoli of goat (Capra hircus). Veterinary World. 2008;1(10):312-313.
24. Bacha WJ, Bacha LM. Color Atlas of Veterinary Histology. 2nd ed. Philadelphia: Lippincott Williams & Wilkins; 2000. p. 162.
25. Bal HS, Ghoshal NG. Morphology of the terminal bronchiolar region of common laboratory mammals. Veterinary Anatomy Department, USA. 1988;22:76-82. https://doi.org/10.1258/002367788780746539